A Linearized Intensity Modulator for Photonic Analog-to-Digital Conversion Using an Injection-Locked Mode-Locked Laser

Edris Sarailou, *Student Member, IEEE*, Abhijeet Ardey, *Student Member, IEEE*, and Peter J. Delfyett, *Fellow, IEEE*

***Abstract*—A linearized intensity modulator for pulsed light based on an injection-locked mode-locked laser (MLL) is presented here. This has been realized by introducing a monolithic Fabry–Pérot MLL into one of the arms of a conventional Mach–Zehnder interferometer (MZI) and injection-locking it to a MLL which is the input to the interferometer. By modulating the current on the gain section or the voltage of the saturable absorber (SA) section of the injection-locked laser, one can introduce an arcsine phase response on each of the injected longitudinal modes. By combining the modulated optical comb with its unmodulated counterpart one can produce a linearized intensity modulator. The linearity of this modulator is inherent in its design and no pre- or postdistortion linearization scheme is utilized. The results of the two-tone intermodulation experiment are presented here for this modulator and a spur-free dynamic range (SFDR) of ~70 dB·Hz$^{2/3}$ is achieved by modulating the voltage of the SA. The reported SFDR is limited by the noise of the MLLs. The dynamic range could be further improved by decoupling the phase modulation and amplitude modulation. The proposed and demonstrated configuration as an analog optical link with improved linearity has the potential to increase the performance and resolution of photonic analog-to-digital converters (ADCs).**

***Index Terms*—Injection-locked lasers, mode-locked lasers, optical intensity modulators, photonic analog to digital converters.**

I. Introduction

PHOTONIC ADCs are desirable for high speed and high performance sampling and digitization of microwave signals. They could potentially eliminate the required mixing and filtering stages of the radio frequency (RF) carriers (down-conversion) used in low speed conventional electrical ADCs and could provide a smaller size and weight, lower cost, wider instantaneous bandwidth, and increased reliability [1], [2].

Photonic sampled ADC based on an analog optical link is becoming a promising approach among the many suggested configurations [3], [4]. $LiNbO_3$ electro-optic modulators are by far the most developed technologies used as optical modulator in analog optical links. The ability to handle high optical powers, low dependency on wavelength and temperature and high modulation bandwidth make the $LiNbO_3$ modulator a very attractive candidate [5]. However being used for photonic ADCs limits the overall performance because of the following two main reasons: 1) The required voltage to get the maximum extinction (V_π) is much higher than the voltage of the RF signal and thus RF amplifier with a high linear response is needed; 2) MZI has an inherent nonlinear transfer function. Among these, the associated nonlinear transfer function affects the resolution the most. To give an example, the created intermodulation tones (because of the nonlinearities) when driving the modulator with 25% depth of modulation limits the effective number of bits (ENOB) of the ADC to less than 4. Operating at a very low depth of modulation also decreases the dynamic range of the modulator significantly and for any significant number of bits, the least significant bit falls below the thermal noise of the photodetector. There have been numerous reports on pre- or post-distortion linearization techniques [6], [7] to increase the SFDR of these modulators, showing 7–8 bits of resolution [8]. An ENOB of 9.8 has been shown in [9] using a very non-uniform quantization technique which incorporates additional components. These techniques make the photonic ADCs more complex and costly and do not achieve the required performance (more than ten effective bits) for many applications such as radar and surveillance.

Recently a linearized optical intensity modulator has been reported [10]. The linearity of this modulator is inherent in its design and potentially could provide a much higher SFDR without the need for any linearization technique. It employs an injection-locked resonant cavity placed in one of the arms of the MZI. When the frequency of the input light (master laser) is inside the locking range of the resonant cavity (slave laser), its frequency locks to the master laser frequency. Based on Adler's equation [11] the induced phase response of the injection-locked slave laser is an arcsine function of the detuning between the resonance frequency of the slave laser and frequency of the master laser, as shown in

$$\varphi_L = \arcsin\left(\frac{\Delta\omega}{\Delta\omega_L}\right) \tag{1}$$

where $\Delta\omega$ is frequency detuning between master and slave laser and $\Delta\omega_L$ is half of the locking range of the slave laser. This equation is the steady state solution of the Adler's equation under weak injection-locking.

By modulating the slave laser, one can induce an arcsine phase response on the injection seed and by combining it with the unmodulated light in the other arm of the MZI in quadrature, the intensity of the output light of the MZI will be directly proportional to the modulating signal. Previously this modulator

Manuscript received May 6, 2014; revised July 3, 2014 and July 28, 2014; accepted July 31, 2014. Date of publication August 5, 2014; date of current version September 17, 2014.

The authors are with the Center for Research and Education in Optics and Lasers, The College of Optics and Photonics, University of Central Florida, FL 32816 USA (e-mail: esarailo@ creol.ucf.edu; aardey@creol.ucf.edu; delfyett@ creol.ucf.edu).

Color versions of one or more of the figures in this paper are available online at http://ieeexplore.ieee.org.

Digital Object Identifier 10.1109/JLT.2014.2345670

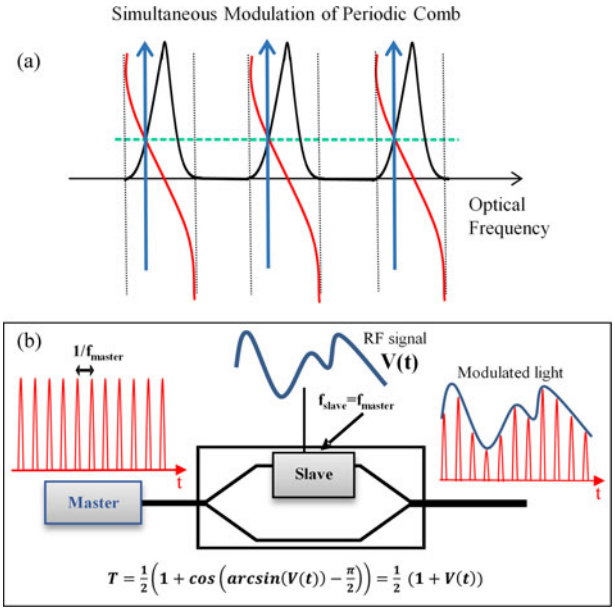

Fig. 1. (Color Online) (a) Schematic showing the slave laser resonances (black), the corresponding phase response (red), injected comb lines from the MLL (blue) and the instantaneous imparted phase on each of the injected comb lines (green). (b) Schematic of the linear interferometric intensity modulator for pulsed light. f_{master} and f_{slave} denote the mode spacing of the master and slave laser, respectively.

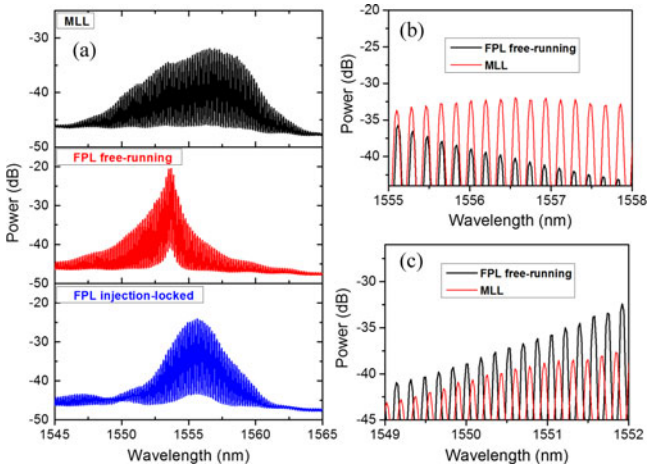

Fig. 2. (Color Online) (a) Optical spectra of the passively MLL (master) and FPL as the resonant cavity before and after injection-locking. Both the lasers are biased with different dc currents to match the frequency spacing between the modes which results in different spectrum widths. The injection-locked FPL spectrum is much narrower than the spectrum of the master MLL since the well-spaced modes of the MLL match at one end of the spectrum with the modes of the FPL as shown in (b) and start to walk off from each other on moving to the other side of the spectrum (c).

concept was implemented using a vertical cavity surface emitting laser (VCSEL) and was shown to provide a very low V_π of 2.6 mV, possible gain, modulation bandwidth of 5 GHz and most importantly SFDR of 120 dB·Hz$^{2/3}$ [10], [12]. However, the above modulator design is limited to single frequency light and to adapt this technique to a pulsed light, a resonant cavity with multiple optical resonances is needed (see Fig. 1(a)). This can be done by using a Fabry-Pérot laser (FPL) as the resonant cavity with multiple resonances and injection-locking them to the frequency comb of the master laser [13]. By modulating the slave laser and inducing an arcsine phase response on each of the injected seeds and by combining them with its unmodulated counterpart from the other arm of the MZI, a linearized intensity modulator for pulsed light can be realized (see Fig. 1(a) and (b)). For injection-locking, there should be an optical spectrum overlap between the lasers and also the free spectral range (FSR) of the FPL should match the pulse repetition rate of the MLL. These conditions could possibly be satisfied if both the MLL laser and the FPL chips are fabricated using the same wafer with the same waveguide structure. However there are two main challenges: (1) two different physical lengths of the lasers are needed (~5–10 μm difference) to compensate for the slight difference in group indices of the FPL and MLL, requiring very accurate device cleaving; (2) because of the dispersion, the optical mode spacing of the FPL is not constant across the spectrum and this makes the injection-locking to all of the equally-spaced optical modes of the MLL more challenging [13]. This is highlighted in the optical spectra of the MLL and FPL, shown in Fig. 2(a)–(c). The optical modes of the two lasers match well at one end of the spectrum (see Fig. 2(b)) and start to walk off from each other on moving to the other side of the spectrum (see Fig. 2(c)). This results in overall poor injection-locking and no induced phase response on the injection-locked resonant cavity.

The frequency shifting of the slave laser necessary to induce the arcsine phase response is expected to be linear with respect to current of the gain section (or the voltage of SA section) within a small locking bandwidth. This is confirmed by measuring the optical frequency shift on a high resolution optical spectrum analyzer while tuning the current of the gain section (not shown here). Furthermore, the 120 dB·Hz$^{2/3}$ SFDR obtained in [12] by utilizing a VCSEL as the resonant cavity suggests a highly linear response in the small locking range.

In this paper, we propose and demonstrate the use of a MLL identical to the master laser as the resonant cavity inside the MZI. This ensures the optical spectrum overlap and ideal matching of the spacing between the optical modes of the lasers. Experimental results of the injection-locking of this laser are presented here. The static phase response of the linearized modulator is presented for different injection power ratios. Instead of just modulating the current on the gain section of the FPL, the use of the MLL as the slave laser gives us two parameters to modulate: the saturable absorber voltage and the current on the gain section. Modulating the current of the gain section leads to carrier density modulation and hence an unwanted amplitude modulation is introduced. However we believe this could be reduced significantly by modulating the SA absorption instead. Experimental results for the signal to intermodulation ratios are presented here and a much reduced third-order intermodulation tone is observed (for the same fundamental RF power) when modulating the SA compared to modulating the gain. Finally the SFDR of this modulator is measured for each of the two above cases.

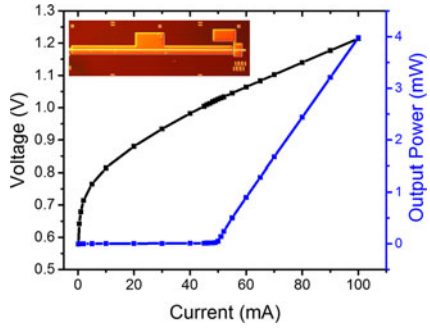

Fig. 3. (Color Online) Typical output power-current and voltage-current characteristics of the MLL operating at 20 °C. No voltage is applied to the SA. The device characteristics are: $I_{\mathrm{threshold}} = 51$ mA, $R = 3.7\,\Omega$ and slope efficiency of 0.077 W/A. Inset shows the top view of the actual fabricated MLL.

II. Injection-Locking of a Passively MLL (Slave) by a Hybridly MLL (Master)

A promising AlGaInAs-InP material system has been used to fabricate the MLL chips. The multiple quantum well structures have been grown on sulfur-doped InP substrate using metal organic vapor phase epitaxy (MOVPE). The active region consists of five compressively strained wells (6 nm thick) and six slightly tensile strained barriers (10 nm thick). Single mode 2.5 μm waveguides are fabricated using standard UV positive lithography process. Wet and dry etching techniques are used to define 1.85 μm deep walls of these vertical mesa waveguides [14]. Benzocyclobutene polymer has been used for planarization to provide robustness and to achieve a lower capacitance in the case of the SA pads. This along with minimizing the SA pad size, enable hybrid mode-locking of the lasers at high frequencies (>20 GHz) [14]. Thermal evaporation is used to fabricate contacts for the SA and gain sections. To provide the electrical isolation between the SA and gain sections, the first two heavily-doped layers in the gap section are removed by a one-step wet etching. The master and slave lasers are chosen to be the adjacent lasers on a laser bar and cleaved simultaneously to obtain the exact same lengths. The total length of the lasers is 1.868 μm with the SA length of 70 μm. The ratio of the SA to gain section length is chosen in such a way that the relaxation oscillations are minimum and the mode-locking quality is the best possible. The facets are left uncoated and the devices are mounted p-side up on gold coated copper studs which themselves sit on top of thermo-electric coolers (TEC). The TEC currents are controlled using high precision proportional-integrated-differential controllers with a stability of 0.001 °C. This is very critical for stable injection-locking since even a 0.001 °C change results in a ~15 MHz drift in the optical frequency and a subsequent change in the quadrature point of the MZI. Fig. 3 shows the electrical and optical characteristics of the MLL when no voltage is applied to the SA. A top view picture of the device is also shown in the inset of Fig. 3. A threshold current of 51 mA, device resistance of 3.7 Ω and slope efficiency of 0.077 W/A is measured from these data.

The master laser is hybridly mode-locked by forward biasing the gain section using a simple dc probe and modulating the reverse-biased SA section. A high speed bias-tee is used to combine the reverse bias voltage and the RF signal. The mixed

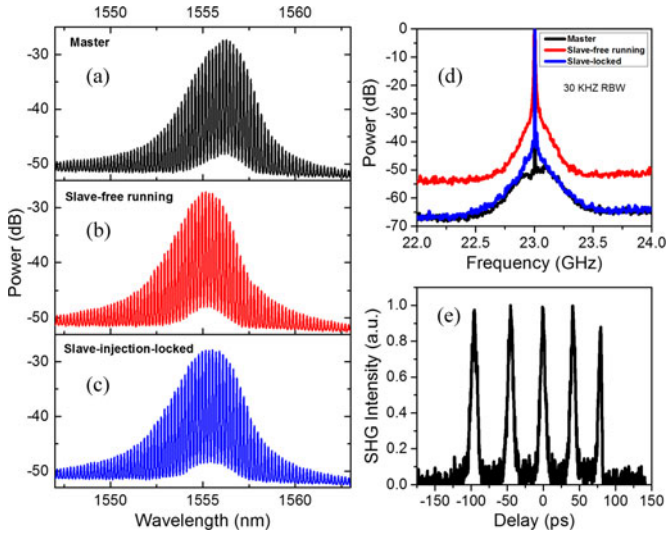

Fig. 4. (Color Online) (a) Optical spectrum of the master laser (black) with $I_{\mathrm{gain}} = 65$ mA, $V_{SA} = -1.8$ V, $T = 20°\mathrm{C}$ and 6 dBm of RF power at 22.998 GHz (b) and (c) optical spectra of the slave laser before (red) and after (blue) injection-locking with $I_{\mathrm{gain}} = 65$ mA, $V_{SA} = -1.9$ V, $T = 19.100°\mathrm{C}$ and injection ratio of −27.8 dB. (d) Normalized RF spectra of the master laser and slave laser before and after injection-locking. (e) Autocorrelation trace of the master laser (slave laser trace is not shown since it is same as that of the master laser with similar pulse width).

signal is applied to the SA using a 40 GHz ground-signal (GS) microwave coplanar probe. The slave laser is passively mode-locked by forward biasing the gain section and reverse biasing the SA section. Bias-tees are used for gain and SA sections to be able to apply the ac signal and modulate them separately. Aspheric lenses are used to couple the light in and out of the lasers. The master laser beam is divided using a non-polarizing beam splitter (BS). An optical isolator with more than 35 dB isolation is used to avoid any reflection being coupled back to the master laser. The injection power is adjusted using a neutral density filter (NDF) and monitored at the same time with the help of a pellicle BS and an optical power meter. The injecting facet is the gain section facet of the slave laser. The output light from the slave is coupled to an SMF fiber and amplified using a semiconductor optical amplifier before going to diagnostics. Fig. 4(a)–(c) show the optical spectra of the master and slave laser before and after injection-locking. Here the master laser is operating at 65 mA of bias current and a reverse bias voltage of −1.8 V and is maintained at a constant temperature of 20 °C. An RF power of 6 dBm at 22.998 GHz is applied to the SA to achieve hybrid mode-locking of the laser. The slave laser is passively mode-locked with 65 mA of bias current and a reverse bias voltage of −1.9 V and the operating temperature of 19.100 °C. Both lasers are running at the same bias currents and the same SA reverse bias voltages to achieve the same spectral width. SA voltages are carefully chosen to match the repetition rate frequencies and the operating temperature of the slave laser is carefully tuned for a precise overlap of its optical modes with that of the master laser. A high resolution optical spectrum analyzer is used to monitor the optical modes in more detail. The power injection ratio is −27.8 dB and is chosen to achieve the best injection-locking with the least amount of relaxation oscillations. The measured 3-dB optical bandwidth is about 2 nm

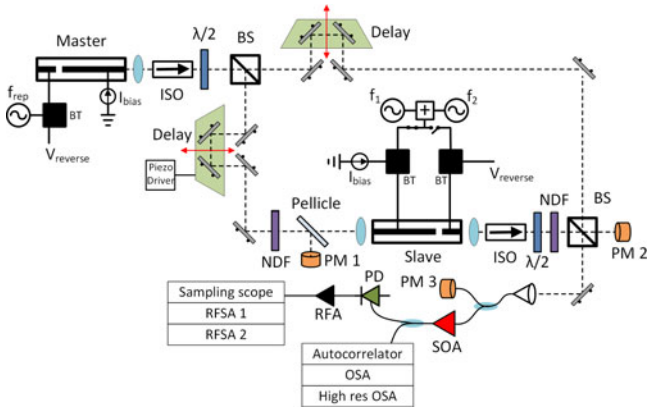

Fig. 5. Experimental setup. ISO: Isolator; BS: Beam splitter; λ/2: Half-wave plate; NDF: Neutral density filter; BT: Bias-Tee; PM: Power meter; SOA: Semiconductor optical amplifier; PD: Photo-detector; RFA: Radio frequency amplifier; OSA: Optical spectrum analyzer; RFSA: Radio frequency spectrum analyzer.

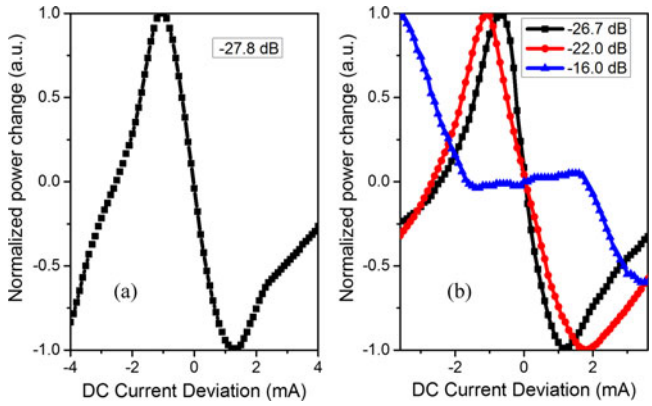

Fig. 6. (a) Normalized change of the output power of the MZI (static phase change) as a function of dc current deviation of the slave laser. Master laser is running with $I_{\rm gain} = 65$ mA, $V_{SA} = -1.8$ V, $T = 20°$C and 6 dBm of RF power at 22.998 GHz. Slave laser is running with $I_{\rm gain} = 65$ mA, $V_{SA} = -1.9$ V and $T = 19.100°$C. Here the power injection ratio was −27.8 dB, (b) Static phase response as a function of dc current deviation for different power injection ratios. The locking bandwidth increases as the injection ratio increases, however by further increasing it, the relaxation oscillations dominate and the injection-locking becomes unstable (−16 dB).

for both lasers. Fig. 4(d) shows the corresponding RF spectra and confirms that the passively mode-locked slave laser follows the hybridly mode-locked master laser. The autocorrelation trace of the pulses from master laser are shown in Fig. 4(e). The pulse width is measured to be ∼5 ps assuming a Gaussian shape and the pulses are 2.8 times transform limit. The autocorrelation trace of the slave laser is not shown here since it is almost identical to that of the master laser.

III. Experimental Setup of the Linearized Intensity Modulator for Pulsed Light

A schematic of the experimental setup is shown in Fig. 5. Free space optical delays are used in both the arms of the MZI to be able to match the path lengths to achieve same pulse overlap after splitting. PZT linear optical stage is used in one of the optical delays to fine-tune the path difference and bias the MZI at quadrature. Power is monitored at three places in the setup: the injected power to the slave laser, the free space power in each of the arms of the interferometer, and the optical power coupled to the fiber from each of the arms. The last two power meters and a NDF placed in front of the slave laser are used to monitor and balance the optical power of each arms and help to increase the visibility of the MZI. With the help of half-wave plates, the polarization of each arm is adjusted to further increase the visibility to ∼68%. Normalized change of the output power (static phase shift response) of the modulator for the power injection ratio of –27.8 dB is obtained by deviating the current of the slave laser around the bias point and monitoring the output power of the MZI (see Fig. 6(a)). Static phase shift of π is achieved when the bias current of the slave laser is changed by approximately 2.3 mA. This corresponds to a full locking-bandwidth of 665 MHz. The effective V_π is calculated to be 8.5 mV. The static phase shift response in the locking range deviates from the expected pure linear response because of the significant amount of PM-to-AM coupling created by modulating the current of the slave laser. The −27.8 dB power injection ratio is chosen to avoid relaxation oscillations which are the byproducts of the injection-locking. Increasing the injection ratio, one could possibly increase the visibility of the interferometer, however this

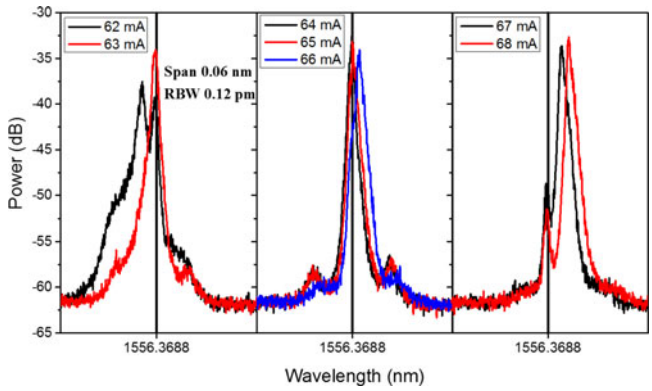

Fig. 7. (Color Online) High resolution optical spectra of the slave laser for different bias currents. The slave remains locked for the bias currents between 64 to 66 mA and unlocks for currents outside of the locking range. The 1 μW injection signal (−27.8 dB of injection ratio when slave is biased at 65 mA) from the master laser is coupled into the slave laser from the gain section facet. Master laser bias current is kept constant at 65 mA. The injection seed from the master laser is at 1556.3688 nm and shown with the vertical solid black line.

itself creates relaxation oscillations and compromises the visibility of the interferometer. Fig. 6(b) shows the static phase response of the modulator for three different injection ratios. An increase in the injection-locking bandwidth is expected as the injection ratio increases. However by further increasing the injection ratio (−16 dBm), relaxation oscillations become dominant and the injection-locking becomes unstable.

Fig. 7 shows the high resolution optical spectra of the slave laser for different bias currents, where 1 μW of optical power from the gain side of the master laser (equivalent to −27.8 dB of power injection ratio) is injected to the slave laser. Here the master laser bias current is kept constant at 65 mA. The injection seed from the master laser is at 1556.3688 nm and shown with a solid black line. The slave follows the master in the approximate current range of ∼64 to 66 mA. As shown in Fig. 7 for the bias currents which are out of the locking bandwidth, the injection-locking becomes unstable and both the slave and master laser outputs are seen inside the slave laser spectra.

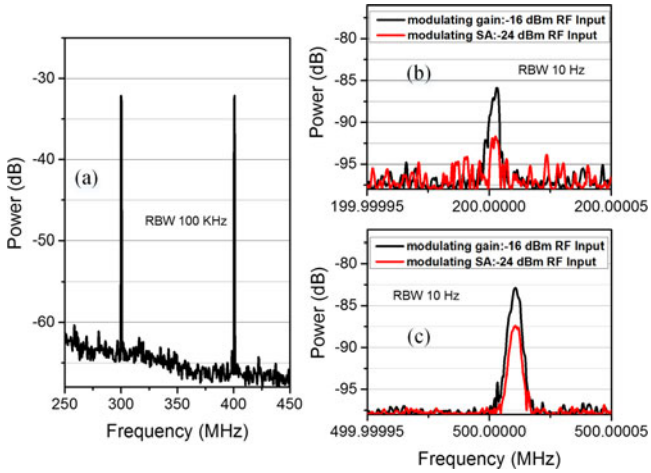

Fig. 8. (Color Online) (a) Photo-detected RF power spectrum of fundamental frequencies for the input RF power of –16 dBm when modulating the gain and −24 dBm when modulating the SA (the input powers are adjusted to achieve the same fundamental powers for comparison). (b) detected RF power spectra of the third-order intermodulation tones at 200 MHz. (c) detected RF power spectra of the third-order intermodulation tones at 500 MHz. Intermodulation tone shown in black when modulating the gain section and shown in red when modulating the SA section.

IV. Two-Tone Intermodulation Experiment

Two-tone intermodulation experiment results are presented in this section as a measure of the linearity of this modulator. The bias point of the modulator is critical since any deviation from the quadrature point would deteriorate the linearity of the modulator. The starting bias point could be off because of the asymmetric locking range of the resonant cavity. This is associated with any semiconductor laser with a non-zero alpha parameter [15]. This issue has been addressed by finding the center point of the static phase response curve and its corresponding bias current (here was 64.7 mA) and readjusting the bias current to this new value. The interferometer is again balanced accordingly.

In order to measure the signal to intermodulation ratio, the modulator (gain section current or saturable absorber voltage) is modulated with two RF signals with the frequencies of 300 and 400 MHz simultaneously. As shown in Fig. 5, the RF signals are combined using a 3-dB coupler and applied to the bias-tee of either gain section or SA section. The photo-detected RF signal of the modulated light is split into two and monitored with two RF spectrum analyzers at the same time; one for fundamental frequencies with a larger frequency span and the other for third-order intermodulation tones at 200 and 500 MHz with a span of 512 Hz. Fig. 8(a) shows the photo-detected RF power spectrum of the fundamental tones. To be able to compare the third-order intermodulation tone when modulating the gain with third-order intermodulation tone when modulating the SA, the input powers to the modulator are adjusted in such a way that the same fundamental powers are seen after photodetection. The applied input RF power was −16 dBm when modulating the gain and –24 dBm when modulating the SA. Fig. 8(b) and (c) show the third-order intermodulation tones at 200 and 500 MHz, respectively. The 500 MHz sideband is used for the calculations since it was the larger spur compared to the 200 MHz sideband. From this data, signal-to-intermodulation ratios of 50.8 and 55.3 dB

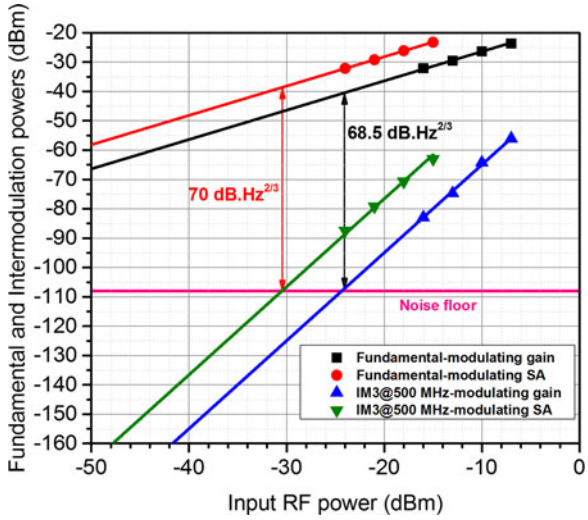

Fig. 9. Fundamental and third-order intermodulation powers as a function of the input RF power to the modulator.

are obtained when modulating the gain and SA, respectively. A ∼4.5 dB improvement is achieved by modulating the voltage of the SA over the gain of the slave laser since modulating the SA would create less AM as opposed to modulating the gain (carrier density) of the slave laser.

Fig. 9 shows the fundamental and third-order intermodulation powers for different input RF powers for each of the gain and SA modulation cases. A linear fit of slope one and another linear fit of slope three are applied to the fundamental and intermodulation tones respectively. Spur-free dynamic range of 68.5 and 70 dB·Hz$^{2/3}$ are obtained from modulating the gain and SA, respectively. Here the SFDR measurement is limited by noise from beating between the relatively broad linewidth laser modes.

V. Discussion

The modulation bandwidth of this modulator is limited by the steady state solution of Adler's equation which suggests that the modulation frequency should be much slower than the repetition rate of the MLL. Assuming a 5% ratio, this would give a modulation bandwidth of about 1.1 GHz for the MLLs used here. The modulator still would operate for higher frequencies, however the phase response would deviate from the arcsine. The bandwidth could be increased by having MLLs with higher repetition rates [16]. This can be realized by having shorter physical length and employing the colliding pulse MLL scheme. This type of modulator with a very high sampling rate could be used for oversampled sigma-delta ADC [17].

The SFDR measurement provided here is limited by noise from beating between the relatively broad linewidth laser modes. This noise extends to higher frequencies as the optical linewidth of the lasers get larger (here about ∼200 MHz). This could be addressed by reducing the overall loss of the cavity such as improving the waveguide design and coating the facets. Also there have been many reports on narrow optical linewidth monolithic MLLs using different material system [18].

Currently available electronic ADCs with similar bandwidth may offer comparable or modestly better SFDR and ENOB to

results reported here. However we believe our novel design has the potential for significantly higher bandwidth and linearity, ultimately providing a superior ENOB compared to electrical samplers of the same bandwidth.

VI. Conclusion

A novel linearized intensity modulator for pulsed light is presented here for the first time. This has been realized by introducing a passively MLL injection-locked to a hybridly MLL (which is the input to the MZI) into one of the arms of the MZI. By modulating the injection-locked laser, one can induce arcsine phase response on each of the injected longitudinal modes. A linear intensity modulator is obtained by interfering the modulated light with its unmodulated counterpart from the other arm in quadrature. A low V_π of 8.5 mV eliminates the need for a linear RF amplifier required for RF signal amplification in the case of $LiNbO_3$ modulator .The current of the gain section or voltage of the SA are used to modulate the slave laser. Modulating the SA provides a reduced AM and hence a reduced third-order intermodulation tone with respect to modulating the gain. A SFDR of 70 dB·$Hz^{2/3}$ is obtained when modulating the SA. The reported SFDR is limited by the noise of the MLLs. Employing this novel linearized modulator in an analog optical link offers the potential to improve the resolution and the overall performance of the photonic sampled ADC.

References

[1] B. L. Shoop, *Photonic Analog-to-Digital Conversion*. New York, NY, USA: Springer-Verlag, 2000.

[2] G. Valley, "Photonic analog-to-digital converters," *Opt. Exp.*, vol. 15, no. 5, pp. 1955–1982, Mar. 2007.

[3] C. H. Cox, III, *Analog Optical Links*. Cambridge, U.K.: Cambridge Univ. Press, 2004.

[4] P. W. Juodawlkis, J. C. Twichell, G. Betts, J. J. Hargreaves, R. D. Younger, J. L. Wasserman, F. J. O'Donnell, K. G. Ray, and R. C. Williamson, "Optically sampled analog-to-digital converters," *IEEE Trans. Microw. Theory Tech.*, vol. 49, no. 10, pp. 1840–1853, Oct. 2001.

[5] G. L. Li and P. K. L. Yu, "Optical intensity modulators for digital and analog applications," *J. Lightw. Technol.*, vol. 21, no. 9, pp. 2010–2030, Sep. 2003.

[6] R. Sadhwani and B. Jalali, "Adaptive CMOS predistortion linearizer for fiber-optic links," *J. Lightw. Technol.*, vol. 21, no. 12, pp. 3180–3193, Dec. 2003.

[7] P. Myslinski, C. Szubert, A. P. Freundorfer, P. Shearing, J. Sitch, M. Davies, and J. Lee, "Over 20 GHz MMIC pre/postdistortion circuit for improved dynamic range broadband analog fiber optic link," *Microw. Opt. Technol. Lett.*, vol. 20, no. 2, pp. 85–88, Jan. 1999.

[8] W. Ng, D. Persechini, D. Yap, S. Morton, C. Fields, and J. Jensen, "Ultra-high speed photonic analog-to-digital conversion techniques," presented at the*Int. Conf. Contemporary Photon.*, Tokyo, Japan, 2002.

[9] R. C. Williamson, R. D. Younger, P. W. Juodawlkis, J. J. Hargreaves, and J. C. Twichell, "Precision calibration of an optically sampled analog-to-digital converter," in *Proc. Dig. IEEE LEOS Summer Top. Meeting Photon. Time/Freq. Meas. Control*, pp. 22–23, Jul. 2003.

[10] N. Hoghooghi, I. Ozdur, M. Akbulut, J. Davila-Rodriguez, and P. J. Delfyett, "Resonant cavity linear interferometric intensity modulator," *Opt. Lett.*, vol. 35, no. 8, pp. 1218–1220, Apr. 2010.

[11] R. Adler, "A study of locking phenomena in oscillators," *Proc. IEEE*, vol. 61, no. 10, pp. 1380–1385, Oct. 1973.

[12] N. Hoghooghi, J. Davila-Rodriguez, S. Bhooplapur, and P. J. Delfyett, "120 dB. $Hz^{2/3}$ spur free dynamic range from a resonant cavity interferometric linear intensity modulator," presented at the *Conf. Lasers Electro-Opt.*, San Jose, CA, USA, May 2012, pp. 1–2.

[13] E. Sarailou, A. Ardey, N. Hoghooghi, and P. Delfyett, "Towards linear interferometric intensity modulator for photonic ADCs using an injection locked AlInGaAs quantum well Fabry–Pérot laser," in *Proc. Conf. Lasers Electro-Opt.*, May 2012, pp. 1–2.

[14] E. Sarailou, A. Ardey, and P. Delfyett, "Low noise ultrashort pulse generation by direct RF modulation at 22 GHz from an AlGaInAs multiple quantum-well laser at 1.55 μm," *IEEE Photon. Technol. Lett.*, vol. 24, no. 17, pp. 1561–1563, Sep. 2012.

[15] F. Mogensen, H. Olesen, and G. Jacobsen, "Locking conditions and stability properties for a semiconductor laser with external light injection," *IEEE J. Quantum Electron.*, vol. 21, no. 7, pp. 784–793, Jul. 1985.

[16] Y. K. Chen, M. C. Wu, T. Tanbun-Ek, R. A. Logan, and M. A. Chin, "Subpicosecond monolithic colliding-pulse mode-locked multiple quantum well lasers", *Appl. Phys. Lett.*, vol. 58, no. 12, pp. 1253–1255, 1991.

[17] B. L. Shoop, "Optical oversampled analog-to-digital conversion," Ph.D. thesis, Stanford Univ., Stanford, CA, USA, 1992.

[18] A. Ardey, J. Kim, E. Sarailou, and P. Delfyett, "Optical and RF stability transfer in a monolithic coupled-cavity colliding pulse mode-locked quantum dot laser," *Opt. Lett.*, vol. 37, no. 17, pp. 3480–3482, 2012.

Edris Sarailou (S'12) received the B.S. degree in electrical and electronic engineering from Semnan University, Semnan, Iran, and the M.Sc. Degree in electrical engineering (electromagnetic waves) from Shiraz University, Shiraz, Iran, in 2004 and 2007, respectively. He is currently working as a Graduate Research Assistant toward the Ph.D. degree in optics at CREOL in Orlando, FL, USA.

From 2005–2007, he was a Graduate Research Assistant working on the first electro-optic switch using an azo nonlinear optical polymer. His main research interests include the monolithic quantum well mode-locked lasers and their applications for photonic analog to digital converters.

Mr. Sarailou is a Student Member of IEEE Photonic Society.

Abhijeet Ardey (S'11) received the B.S. and M.S. degrees in physics from University of Delhi, Delhi, India, in 2001 and 2003, respectively, and the M.S. degree in physics from University of Central Florida (UCF), Orlando, FL, USA, in 2007. He is currently working toward the Ph.D. degree in physics at the Center for Research and Education in Optics and Lasers, UCF.

He is currently a Graduate Research Assistant at the Center for Research and Education in Optics and Lasers, UCF.

His research interests include the development of novel low noise mode-locked semiconductor lasers. He is involved with the device design/fabrication and development of both chip-scale and external cavity III–V based semiconductor lasers for applications in future high capacity optical communication networks.

Peter J. Delfyett (S'79–M'94–SM'96–F'02) received the Ph.D. degree in electrical engineering from the City University of New York, New York, NY, USA, in 1988. He is the University of Central Florida Trustee Chair Professor of Optics, EE, and Physics, The College of Optics and Photonics, and the Center for Research and Education in Optics and Lasers, University of Central Florida. Prior to this, he was a Member of the Technical Staff at Bell Communications Research from 1988–1993.

Dr. Delfyett served as the Editor-in-Chief of the *IEEE Journal of Selected Topics in Quantum Electronics* (2001–2006), and served on the Board of Directors of the Optical Society of America. He served as an Associate Editor of IEEE Photonics Technology Letters, and was the Executive Editor of IEEE LEOS Newsletter (1995–2000). He is a Fellow of the Optical Society of America, Fellow of IEEE Photonics Society, and Fellow of the American Physical Society. He was also a Member of the Board of Governors of IEEE-LEOS (2000–2002) and a Member of the Board of Directors of the Optical Society of America (2004–2008). In addition, he received the National Science Foundation's Presidential Faculty Fellow Early Career Award for Scientists and Engineers, which is awarded to the Nation's top 20 young scientists. He has published more than 650 articles in refereed journals and conference proceedings, has been awarded 35 United States Patents. He received the University of Central Florida's 2001 Pegasus Professor Award which is the highest honor awarded by the University. He has also endeavored to transfer technology to the private sector, and helped to found "Raydiance, Inc.," which is a spin-off company developing high power, ultrafast laser systems, based on his research, for applications in medicine, defense, material processing, biotech, and other key technological markets. Most recently, he received the APS Edward Bouchet Award for his significant scientific contributions in the area of ultrafast optical device physics and semiconductor diode based ultrafast lasers, and for his exemplary and continuing efforts in the career development of underrepresented minorities in science and engineering.